T.C.
BOLU ABANT İZZET BAYSAL ÜNİVERSİTESİ
INSTITUTE OF GRADUATE STUDIES
DEPARTMENT OF CHEMISTRY

SYNTHESIS AND CHARACTERIZATION OF KOTOITE-TYPE NICKEL BORATE NANOPARTICLES

MASTER OF SCIENCE, CHEMISTRY

ERAY SÖNMEZER

THESIS SUPERVISOR
Prof. Dr. Ayşe MORKAN

BOLU, OCTOBER 27

ACCEPTANCE AND APPROVAL PAGE

SYNTHESIS AND CHARACTERIZATION OF KOTOITE-TYPE NICKEL BORATE NANOPARTICLES

submitted by **Eray SÖNMEZER** in partial fulfillment of the requirements for the degree of **Master of Science** in Department of **CHEMISTRY** with unanimity/majority vote is hereby approved. 10/27/2025

Jury Members	**Signature**
Supervisor Prof. Dr. Ayşe MORKAN Bolu Abant Izzet Baysal University	.....
Member Prof. Dr. Fazilet Devrim ÖZDEMİRHAN Bolu Abant Izzet Baysal University	.....
Member Prof. Dr. Mecit AKSU Düzce University	.....

Institute of Graduate Studies Approval

Prof. Dr. İbrahim KÜRTÜL

Director of Institute of Graduate Studies

ETHICAL STATEMENT

In this thesis study, which I have prepared in accordance with Bolu Abant İzzet Baysal University, Institute of Graduate Studies' Thesis Writing Guide and Template;

- I have obtained the data, information and documents presented in the thesis within the framework of academic and ethical rules,
- I have presented all information, documents, evaluations, and results in accordance with the rules of scientific ethics and morality,
- I have cited and referenced all the works I have benefited from in the thesis study,
- I have not made any changes to the data used,
- I declare that the work I have presented in this thesis is original, and in any other case, I declare that I accept all loss of rights that may arise against me.

According to the similarity report obtained by applying the filters determined by the directorate of the institute in the Turnitin program related to the thesis, the similarity index of the thesis does not exceed 30%.

.....

ERAY SÖNMEZER

PREFACE

This thesis represents the culmination of a long and meticulous research process. The study focuses on the "**Synthesis and characterization of kotoite-type nickel borate nanoparticles**, a topic that reflects both my personal interest and scientific curiosity. The findings presented in this work were obtained through extensive experimentation, careful analysis, and systematic evaluation. This research aims to contribute to the existing body of knowledge in the field and to provide new perspectives for a deeper understanding of the properties of kotoite-type nickel borate nanoparticles.

Eray SÖNMEZER
10/27/2025

.

ABSTRACT

SYNTHESIS AND CHARACTERIZATION OF KOTOITE-TYPE NICKEL BORATE NANOPARTICLES
MSC THESIS
ERAY SÖNMEZER
BOLU ABANT IZZET BAYSAL UNIVERSITY
INSTITUTE OF GRADUATE STUDIES
DEPARTMENT OF CHEMISTRY
(SUPERVISOR: PROF. DR. AYŞE MORKAN)

BOLU, 27 OCTOBER 2025
xiii + 39

In this study, the synthesis and characterization of nickel borate ($Ni_3(BO_3)_2$) nanoparticles were investigated. The materials were prepared using two different organic fuels, tartaric acid and hexamethylenetetramine (HMTA) via the solution combustion synthesis (SCS) method. Nickel nitrate and boric acid were used as the precursor materials, and the reaction conditions were carefully optimized based on stoichiometric calculations.

The resulting products were calcined at 400°C and 900°C and thoroughly characterized. X-ray diffraction (XRD) analyses confirmed the successful formation of $Ni_3(BO_3)_2$ nanoparticles with both fuel types. Fourier-transform infrared (FTIR) spectroscopy revealed the characteristic vibration bands of the BO_3 units.

The results demonstrated that both the choice of fuel and the calcination temperature play a significant role in determining the crystalline structure and thermal stability of the products. Nickel borates synthesized with tartaric acid exhibited greater structural stability at higher temperatures, whereas HMTA-derived (hexamethylenetetramine) samples showed more efficient performance at lower temperatures.

These findings provide valuable insights for the effective optimization of nickel borate nanoparticles in industrial applications and serve as a useful reference for future research in this area.

KEYWORDS: Nickel Orthoborate, Solution Combustion Synthesis(SCS), Tartaric Acid, HMTA, XRD, FTIR

ÖZET

KOTOİT TİPİNDE NİKEL BORAT NANOPARÇACIKLARIN SENTEZİ VE KARAKTERİZASYONU
YÜKSEK LİSANS TEZİ
ERAY SÖNMEZER
BOLU ABANT İZZET BAYSAL ÜNİVERSİTESİ
LİSANSÜSTÜ EĞİTİM ENSTİTÜSÜ

KİMYA ANA BİLİM DALI
(TEZ DANIŞMANI: PROF. DR. AYŞE MORKAN)

BOLU, 27 EKİM 2025
xiii + 39

Bu çalışmada, nikel borat ($Ni_3(BO_3)_2$) nanoparçacıklı malzemelerin sentezi ve karakterizasyonu incelenmiştir. Malzemeler, iki farklı organik yakıt—tartarik asit ve hexamethylenetetramine (HMTA)—kullanılarak çözeltide yanma yöntemi (solution combustion synthesis, SCS) ile hazırlanmıştır. Başlangıç maddeleri olarak nikel nitrat ve borik asit tercih edilmiş ve reaksiyon koşulları stokiyometrik hesaplamalar doğrultusunda titizlikle optimize edilmiştir.

Elde edilen ürünler 400°C ve 900°C'de kalsine edilerek detaylı bir şekilde karakterize edilmiştir. X-ışını difraksiyonu (XRD) analizleri, her iki yakıt türü ile de $Ni_3(BO_3)_2$ nanoparçacıklarının başarılı bir şekilde oluştuğunu doğrulamıştır. Fourier dönüşümlü kızılötesi (FTIR) spektroskopisi, BO_3 birimlerine ait karakteristik titreşim bantlarını ortaya koymuştur.

Sonuçlar, hem yakıt türünün hem de kalsinasyon sıcaklığının ürünlerin kristal yapısı ve termal kararlılığı üzerinde önemli bir rol oynadığını göstermiştir. Tartarik asit ile sentezlenen nikel boratlar, yüksek sıcaklıklarda daha kararlı yapılar sergilerken; HMTA (hexamethylenetetramine) kaynaklı örnekler, düşük sıcaklıklarda daha verimli performans göstermiştir.

Bu bulgular, nikel borat nanoparçacıklı malzemelerin endüstriyel uygulamalarda etkin bir şekilde optimize edilmesine yönelik önemli bilgiler sağlamaktadır ve gelecekteki araştırmalar için değerli bir referans niteliği taşımaktadır.

ANAHTAR KELİMELER: Nikel Borat, Çözeltide Yanma Sentezi, Tartarik Asit, HMTA, XRD, FTIR.

TABLE OF CONTENTS

Page

LIST OF FIGURES

Page

LIST OF TABLES

Page

LIST OF PHOTOS

Page

LIST OF ABBREVIATIONS AND SYMBOLS

FTIR : Fourier Transform Infrared
HMTA : Hexamethylenetetramine
TA : Tartaric Acid
SCS : Solution Combustion Synthesis
UV-VIS : Ultraviolet-Visible
XRD : X-Ray Diffraction

ACKNOWLEDGEMENT

I would like to express my deepest gratitude to my esteemed advisor, **Prof. Dr. AYŞE MORKAN**, for her guidance, unwavering dedication, honest advice, constructive criticism, constant encouragement, and profound knowledge throughout my master's studies.

I extend my sincere thanks and respect to **Fatma YALÇIN** for her invaluable help and support during my research. I am deeply grateful to **Dr. Gülden ÖZEN KAHVECİ** for her assistance with the X-ray studies.

Additionally, I would like to express my heartfelt gratitude to my beloved family, my spouse, and my precious daughter for their love, encouragement, and unwavering support throughout my thesis process.

1. INTRODUCTION

Boron has been utilized by human civilizations for thousands of years, ranging from ancient glass and ceramic production to contemporary high-tech applications. Its unique properties, including high thermal stability, neutron absorption capability, and hardness, make boron applicable in various industrial and technological fields. Today, boron plays a significant role in advanced materials, nuclear technology, agriculture, and electronics (Republic of Türkiye Ministry of Energy and Natural Resources, 2024).

Türkiye possesses a substantial portion of the world's boron reserves, holding a noteworthy position in the global boron landscape (Eti Maden, n.d.). These reserves are concentrated in key mining regions such as Eskişehir-Kırka, Kütahya-Emet, Balıkesir-Bigadiç, and Bursa-Kestelek, offering both economic and strategic advantages. In particular, Türkiye's boron deposits are rich in the ^{10}B isotope, which is important for nuclear applications (DergiPark, 2025).

In recent years, global demand for boron and boron-based compounds has increased due to technological developments in electronics, energy storage, and renewable energy sectors. Türkiye's boron resources provide potential support for the country's industrial and commercial activities in this field (Anadolu Agency, 2025).

For these reasons, studies and research on boron are of considerable importance from both scientific and industrial perspectives.

1.1 BORON

Boron is an element found in nearly a hundred different minerals in nature and forms a wide range of chemical compounds. Its atomic number is 5, and its atomic mass is approximately 10.811 atomic mass units. Classified in Group 13 (IIIa) of the periodic table, boron has the electron configuration $1s^2\ 2s^2\ 2p^1$. Boron does not occur freely in nature; it primarily combines with oxygen to form borate minerals such as borax and colemanite. In its crystalline form, boron is hard and brittle, exhibiting semiconductor properties, while its amorphous form appears as a gray powder with very low electrical conductivity. Boron's strong tendency to form

bonds with oxygen allows it to create a wide variety of compounds, ranging from simple molecular structures to complex three-dimensional networks, making boron chemistry a specialized field within materials science.

In nature, boron exists as two stable isotopes, ^{10}B and ^{11}B. The ^{10}B isotope accounts for approximately 19.9 %, while ^{11}B makes up around 80.1 %. Variations in isotope ratios and differences in chemical reactivity serve as important indicators for understanding the formation conditions of boron-containing minerals and isotopic fractionation processes (Britannica, 2025).

Among its crystalline forms, boron is noted for its hardness, ranking second only to diamond, and exhibits complex icosahedral bonding arrangements in many of its polymorphs. When heated in air to approximately 700 °C, boron oxidizes to form boron trioxide (B_2O_3), and at temperatures above 900 °C, it reacts with nitrogen to form boron nitride (BN). Boron nitride is widely used in high-temperature and electronic applications due to its thermal stability and electrical insulating properties (Britannica, 2025).

Due to these properties and its wide range of applications, research on boron holds significant importance from both scientific and industrial perspectives.

Industrial and Agricultural Applications and Türkiye's Position in the Global Boron Market

Boron and its compounds are widely used across numerous industrial and agricultural sectors due to their unique chemical and physical properties. In metallurgical processes, boron functions as an oxygen and gas scavenger and contributes to the production of special alloys and high-performance steels used in automotive and structural applications (Demiral Kurtuluş & Güler, 2003). Boron carbide, a boron compound with exceptional hardness, is utilized in abrasive materials, wear-resistant components, and as a neutron absorber in nuclear power plants and shielding systems (European Borates Association [EBA], 2011). Borate compounds are also applied in glass and ceramics manufacturing, semiconductor production, construction materials, and high-density concretes, while certain boron derivatives serve as catalysts and micronutrients in agriculture (Republic of Türkiye Ministry of Energy and Natural Resources, 2024). These diverse applications

highlight boron's importance in both industrial manufacturing and agricultural productivity.

Türkiye holds a dominant position in the global boron market, possessing approximately 73 % of the world's known boron reserves and ranking second worldwide in boron ore production after the United States (Kar, Sen, & Demirbaş, 2006; Sokmen & Büyükakinci, 2018). The country's deposits, primarily located in western Anatolia, are managed by state-owned enterprises such as Eti Maden, which oversees the extraction and processing of borate minerals (Republic of Türkiye Ministry of Energy and Natural Resources, 2024). Considering that around 53 % of global boron ore deposits and 42 % of global boron production are concentrated in Türkiye, the nation's strategic role in supplying raw boron materials for advanced industrial applications is evident (Kar, Sen, & Demirbaş, 2006; EBA, 2011).

Figure 1.1 Elemental boron appearance

1.1.1 Historical Development and Discovery of Boron

The historical use of boron compounds dates back to ancient civilizations. Archaeological evidence indicates that boron-containing minerals were utilized as early as the 2000s BCE. For instance, the Babylonian civilization imported boron compounds from the Far East for use in gold refining processes (Helvacı, 2019). The ancient Egyptians also exploited boron

minerals in mummification, medical applications, and metalworking techniques (Helvacı, 2019; Britannica, 2025).

During the Middle Ages, particularly in the 8th century, borax became an important commercial commodity in the Arab world. Historical records show extensive use of borax in the Mecca and Medina regions, and Arab scientists produced medicinal compounds from boron salts as early as 875 CE (Helvacı, 2019). Tibet's salt lakes are believed to have been the primary source of borax, which was transported via caravan routes across the Himalayas into India. Borax was subsequently introduced to Europe in the 13th century by the explorer Marco Polo (Bengisu, 2016).

The systematic scientific study and industrial production of boron began with the advancement of modern chemistry. In 1771, sassolite (H_3BO_3) was discovered in the geysers of Tuscany, Italy, marking a major milestone in boron chemistry (Helvacı, 2019). The Industrial Revolution facilitated the large-scale production of boron, with boric acid production commencing in Italy in 1830 and borax mining in Chile beginning in 1852. The discovery of rich boron deposits in California and Nevada in 1864 established the United States as a major global producer (Kar, Sen, & Demirbaş, 2006).

The isolation of elemental boron in the early 19th century was a significant scientific achievement. French chemists Joseph Louis Gay-Lussac and Louis Jacques Thénard, along with British scientist Sir Humphry Davy, succeeded in producing pure boron by reacting boric acid with potassium. Today, boron is predominantly produced by heating borax ($Na_2B_4O_7 \cdot 10H_2O$) with carbon (Bengisu, 2016; Britannica, 2025).

This historical progression demonstrates the long-standing significance of boron, highlighting its continuous use from ancient civilizations to modern industrial applications. Boron compounds have historically served diverse purposes, and they continue to retain strategic and industrial importance today (Helvacı, 2019; Britannica, 2025).

1.1.2 Properties of the Boron Element and Türkiye's Strategic Position

Boron is a chemically versatile element found in nature in the form of multiple isotopes, the most abundant and stable being ^{10}B and ^{11}B, which occur naturally in approximate proportions of 19–20 % and 80–81 %, respectively. The ^{10}B isotope is particularly significant due to its high thermal neutron absorption capacity, making it invaluable in nuclear technology, such as in control rods and radiation shielding (Tunçbilek & Nas, 2025).

Türkiye's Boron Potential

Türkiye holds a prominent position in the global boron market, containing approximately 73 % of the world's known boron reserves. These reserves are especially rich in ^{10}B isotope, enhancing their strategic value for nuclear and high-tech applications (Eti Maden, n.d.). Current estimates suggest that Türkiye's boron reserves are sufficient to sustain production for the next 250–500 years, depending on extraction rates and technological advances (AA, 2025). The primary boron deposits are located in Eskişehir (Kırka), Kütahya (Emet), Balıkesir (Bigadiç), and Bursa (Kestelek), and they include significant amounts of minerals such as tincal, colemanite, and ulexite (Eti Maden, n.d.).

Global Perspective

Compared to other boron-producing countries, where the economic lifespan of boron reserves is estimated at around 50 years, Türkiye's extensive deposits provide a markedly different scenario. The country is poised to become the world's leading and potentially sole significant boron supplier within the next 50–80 years. While the total reserves were initially estimated at 600 million tons in the 1970s, more recent assessments suggest a total of approximately 3 billion tons, reflecting ongoing exploration and re-evaluation (Republic of Türkiye Ministry of Energy and Natural Resources, 2024).

This strategic abundance not only secures Türkiye's role in nuclear technology but also positions it as a major player in other industrial applications such as high-strength ceramics, glass, fiberglass, detergents, and agricultural products. Efficient extraction and processing of these resources into high-value

boron-based materials present a critical opportunity for the national economy and the development of high-technology industries (Helvacı, 2019; Bengisu, 2016).

Moreover, Türkiye's dominance in boron production allows for strategic geopolitical influence, as boron is considered a critical raw material in multiple advanced industrial sectors worldwide. Investments in research, processing technologies, and sustainable mining practices could enhance the value of these resources while maintaining their availability for future generations.

Table 1.1 Global Boron Reserve Shares

Countries	Total Reserve (Thousand ton B203)	Distribution (%)
Turkey	948,712	73,4
USA	80,000	6.2
Russia	100,000	7.7
China	36,000	2.8
Peru	22,000	1.7
Argentina	9,000	0.7
Bolivia	19,000	1.5
Chile	41,000	3.2
Kazakhstan	15,000	1.2
Serbia	21,000	1.6
TOTAL	**1,291.712**	**100**

1.1.3 Industrial-Agricultural Application and Usage Areas of Boron

Glass Industry

Boron compounds are most widely used in the glass manufacturing sector (with a 52% share) for industrial applications. Boron oxide (B_2O_3) compound is primarily used as a basic component in the production of:

- High heat-resistant borosilicate glasses
- Textile and insulation grade glass fibers

- Special laboratory glass materials.

Inorganic glasses based on boron element have emerged as prominent materials for bone tissue applications. Naturally present in the human body (3-20 mg), boron has been clinically proven to play an active role in bone metabolism and wound healing processes.

Key biomedical advantages of these glasses:

- Tissue-friendly chemical reactivity
- Controlled thermal expansion behavior
- Bone-like mechanical properties
- Bioactive ion release capacity

In tissue engineering, borate glasses provide an ideal environment for bone regeneration. They are successfully used in bone defect treatments and implant coatings. Their biocompatibility and osteogenic (bone-forming) effects make them viable alternatives to traditional materials**.**

Borate glasses offer broad application possibilities in the field of photonics. In addition to high optical transparency, density, and mechanical durability, they exhibit excellent transmission properties in the infrared region. They also serve as an economical alternative due to their suitable bandwidth and corrosion resistance. These glasses are preferred in various photonic applications, such as optical amplifiers and laser systems. Furthermore, thanks to their nonlinear refractive index and absorption coefficients, they are among the promising materials for fiber optic communication technologies. (Mariselvam, K., & Arun Kumar, R. , 2016).

Role in the Cleaning Industry

Boron minerals hold a significant place in cleaning products due to their chemical properties:

- Antimicrobial (antiseptic) effect
- Ability to soften hard water
- Stain-bleaching property

These qualities ensure boron's widespread use in soap and detergent formulations.

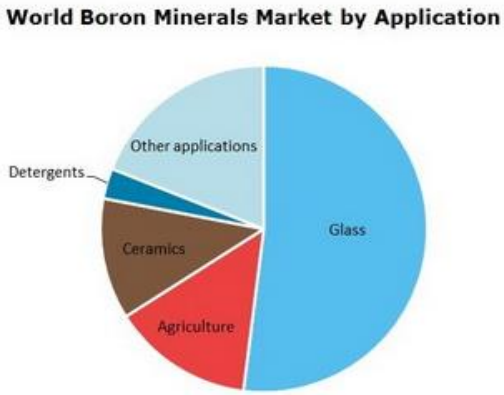

Figure 1.2 Sectoral Distribution of Boron Uses

Fire Safety Applications

Boron derivatives are finding increasing use as flame retardants in various materials:

- Wood and wood products
- Cellulose-based insulation materials
- PVC and textile products

The fire-retardant mechanism of boron is based on forming a protective layer on the flammable surface, thereby cutting off contact with oxygen.

Agricultural Benefits

Research on plant physiology reveals the positive effects of boron on agricultural productivity:

A) In Vegetables:

Growth-accelerating effect

- Noticeable improvement in product quality
- No chemical degradation

B) In Fruit Trees:

- Flowering efficiency
- Fruit set rates
- Fruit quality parameters

Recent studies show that foliar boron applications can increase yields by 15-25% in certain fruit types. These application areas highlight the strategic importance of boron compounds in both industrial and agricultural production. The

widespread use of boron is expected to further expand, especially with the development of environmentally friendly and sustainable production techniques.

Boron stands out as an important element with its versatile properties in both strengthening composite materials and ensuring fire safety. Although boron-containing composites, reinforced with boron fibers and polymer resins, offer high performance, the high production cost of boron fibers can limit their application areas.

Different boron compounds, especially sodium borohydride, find a wide range of industrial applications. Sodium borohydride, widely used commercially and known as a hydrogen carrier/storage material, is utilized in various processes such as paper bleaching, reducing textile waste, and removing heavy metals from wastewater.

Mineral	Formula	B_2O_3 (%)	Regions of mineral
Kernite (Rasortie)	$Na_2B_4O_7.4H_2O$	51.0	Kırka, USA, and Argentina
Pandermite (Priceite)	$CaB_{10}O_{19}.7H_2O$	49.8	Sultancayır and Bigadic
Ulexite (Boronatrocalcite)	$NaCa\ B_5O_9.8H_2O$	43.0	Kırka, Bigadic, Emet, and Argentina
Colemanite	$Ca_2B_6O_{11}.5H_2O$	50.8	Emet, Bigadic, Kucukler, and USA
Probertite (Kramerite)	$NaCaB_5O_9.5H_2O$	49.6	Kestelek, Emet, and USA
Szaibelyite (Ascharite)	$MgBO_2.2OH$	41.4	Russia
Boraxs (Tincal)	$Na_2B_4O_7.10H_2O$	36.6	Kırka, Emet, Bigadic, and USA
Boracite (Stassfurite)	$Mg_6B_{14}O_{26}C_{12}$	62.2	Germany
Hydroboracite	$CaMgB_6O_{11}.6H_2O$	50.5	Emet

Figure 1. 3 Commonly Used Boron Minerals Worldwide (Kar, Y., Sen, N., & Demirbaş, A. (2006).

The Role of Boron in Boron and Polymer Composites: Flame Retardancy and Application Areas

Boron stands out as a crucial element with its versatile properties, playing a significant role in both strengthening composite materials and enhancing fire safety. Boron-containing composites, composed of polymer resins reinforced with boron fibers, offer high performance; however, the high production cost of boron fibers can limit their application areas.

Various boron compounds, particularly sodium borohydride, find extensive use across a wide industrial spectrum. Sodium borohydride, widely used commercially and known as a hydrogen carrier/storage agent, is utilized in diverse

processes such as paper bleaching, textile waste reduction, and heavy metal removal from wastewater (Sokmen, N., & Büyükakinci, B. Y. , 2018).

Flame Retardant Properties of Boron Compounds

Boron's flame retardant effect stems from its superior properties, such as a high autoignition temperature (510-525°C), inspiring much research on this topic. Boron compounds like zinc borate, boric acid, and fluoroborate are among the most frequently preferred flame retardant agents. These compounds also stand out for being environmentally friendly; they do not cause toxic gas emissions and exhibit low volatility.

The mechanism of action for boron-based flame retardants is quite interesting: they form a glass-like protective layer on the burning material. This layer acts as a barrier against the oxidation of polymer chains, cutting off contact with oxygen and thus suppressing combustion. The use of boron compounds as flame retardants in the textile sector is also becoming increasingly widespread.

With increasing industrialization, dense residential areas, and advancing technology, the rising risk of fires is increasing the demand for flame-protective textile products. Statistical analyses indicate that boron compounds significantly improve the flame retardancy quality of fabrics, and borax has been determined to provide the most effective results in this regard. Furthermore, it has been observed that highly effective results in flame retardancy performance are achieved by applying boron compounds along with nitrogen to cellulosic fabrics. Similarly, studies have been conducted on imparting flame retardant properties to propylene and epoxy-based composites by adding various boron compounds.

Consequently, it is observed that the flame retardancy properties are enhanced and LOI (Limited Oxygen Index) values are increased when polymers such as polystyrene, poly(vinyl alcohol), and epoxy (Ethylene-Co-vinyl alcohol) are modified with boron-containing reactive groups. These developments reveal that boron not only enhances the durability of composite materials but also plays a critical role in the field of fire safety (Sokmen, N., & Büyükakinci, B. Y. , 2018).

1.2 BORATES and USES FOR BORATES

1.2.1 Borates

Borates are compounds containing boron and oxygen, classified according to their boron-oxygen units. They are fundamentally divided into three groups:

- Metaborates (BO_3 triangles)
- Tetraborates (B_4O_7 units)
- Pentaborates (B_5O_{10} units)

In these compounds, boron atoms can bond with oxygen atoms in triangular (BO_3) or tetrahedral (BO_4) forms. The structural diversity of borates enables their use in various applications. For example, they are widely utilized in industrial fields such as glass, ceramics, and cleaning materials.

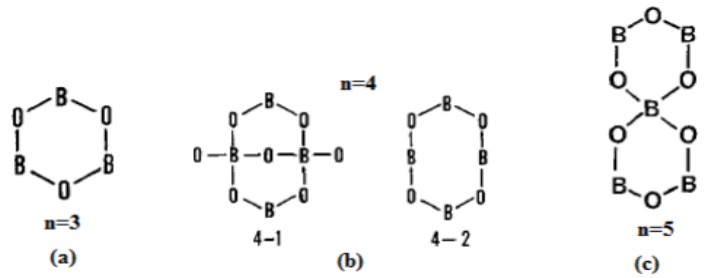

Figure 1.4 **a)** Metaborates **b)** Tetraborates **c)** Pentaborates

1.2.2 Orthoborates:

Orthoborates are compounds containing isolated BO_3^{3-} or BO_4^{5-} ions, with a boron-to-oxygen ratio of 1:3. Structurally, they resemble nitrates and carbonates. Their general formula is MBO_3 (M: metal). For example, orthoborates containing rare-earth elements ($LnBO_3$) exhibit isomorphic structures with calcite ($CaCO_3$).

1.2.3 Metal Borates:

Metal borates are compounds with the general formula $M_3(BO_3)_2$ (M: Mg, Co, Ni, etc.). Their most common natural examples are the minerals kotoite ($Mg_3(BO_3)_2$) and jimboite ($Mn_3(BO_3)_2$). These compounds can be synthesized via solid-state reactions at high temperatures and generally crystallize in the orthorhombic crystal system (Sofronova, S. N., & Nazarenko, I. I., 2019).

a) **b)**

Figure 1.5 **a)** Kotoite **b)** Jimboite

1.2.4 Nickel Borate

Research on metal borates has been actively pursued for over a decade due to their remarkable nonlinear optical properties, lubricating capabilities, flame retardancy, laser applications, and significant magnetic, catalytic, electrochemical, and phosphorescent characteristics. Among various metal borates, nickel borate ($Ni_3B_2O_6$) has attracted growing research interest for its excellent properties and has been utilized in electrochemical capacitors, antimicrobial applications, and as electrocatalyst (Liang, P., Du, L., Wang, X., & Liu, Z.-H., 2014).

Although **$Ni_3B_2O_6$** was first mentioned in early materials research, studies on the synthesis of nickel borate micro- and nanostructures remain relatively limited (Singh, Srinivas, & Ram, 2008). Analysis of the temperature dependence of magnetic susceptibility has revealed that $Ni_3(BO_3)_2$ is a collinear antiferromagnet with a Néel temperature (T_n) of approximately 46 K (Pisarev et al., 2015).

Recent studies have demonstrated controlled synthesis of $Ni_3(BO_3)_2$ nanostructures with various morphologies. For example, Ganguly et al. (2011) synthesized anisotropic nickel borate nanostructures with controlled size and morphology using a microemulsion method. Pang et al. (2011) prepared $Ni_3B_2O_6$ nanoribbons via a simple high-temperature solid-state reaction and examined their antimicrobial, electrochemical, and electrical characteristics. Sun et al. (2022) fabricated $Ni_3(BO_3)_2$ nanospheres via electrodeposition on titanium mesh, demonstrating enhanced electrochemical performance for energy storage.

Additionally, Yamamoto, Miyata, and Koyama (2006) determined the standard Gibbs formation energy for $Ni_3B_2O_6$ using electromotive force measurements with solid electrolytes.

These studies collectively highlight the ongoing interest in $Ni_3(BO_3)_2$ as a functional material, with properties relevant to magnetic, optical, and electrochemical applications, while emphasizing the need for further research into controlled synthesis of nanoscale structures.

Various borate-based cathode materials for lithium-ion batteries, including $Fe_3B_2O_6$, $FeBO_3$, $Cu_3B_2O_6$, $Co_3B_2O_6$, and $M_3B_2O_6$ (M = Co, Ni, Cu), have been investigated due to their cost-effectiveness, low weight, and environmentally friendly characteristics (Sanglay, Garcia, Palaganas, Sorolla, See, Limjuco, & Ocon, 2022). Early studies on iron(III) borates, such as $FeBO_3$ and $Fe_3B_2O_6$, demonstrated their potential as cathode materials and highlighted the suitability of borate frameworks for Li^+ intercalation processes. Despite these findings, the synthesis and detailed characterization of nickel borate ($Ni_3(BO_3)_2$) with controlled particle size and morphology remain relatively unexplored, indicating a promising area for future research. The unique structural versatility of borates, ranging from simple molecular units to complex three-dimensional frameworks, could enable tailored electrochemical performance in Li-ion batteries, making $Ni_3(BO_3)_2$ a potential candidate for high-performance cathode applications.

The $Ni_3(BO_3)_2$ crystal adopts the orthorhombic kotoite structure and belongs to the Pnnm space group, with *two formula units per unit cell* (Pisarev et al., 2015; Effenberger & Pertlik, 1984). In this structure, the six magnetic Ni^{2+} ions are distributed over two crystallographically distinct sites (2a and 4f), each coordinated by distorted NiO_6 octahedra that share edges and corners to form a three-dimensional network. The boron ions are located within trigonal BO_3 groups positioned between the Ni–O octahedra, creating a robust framework that links the metal centers (Pisarev et al., 2015; Effenberger & Pertlik, 1984).

These structural features give rise to extended chains of NiO_6 octahedra along specific crystallographic directions, and BO_3 groups form triangular motifs within the framework that can influence magnetic interactions. Because the Ni^{2+} ions occupy geometrically distinct positions and interact through these

interconnected octahedral and triangular arrangements, competing antiferromagnetic exchange paths may occur, potentially leading to magnetic frustration effects in the system at low temperatures (Pisarev et al., 2015).

In the image of the kotoite structure provided in Figure 1.6, chains extending in triangular groups along the *bc*-plane are highlighted with thick lines. A distinctive feature of this structure is the ribbon-like formations composed of triangular clusters of Ni ions running along the *b*-axis. If the exchange interactions within these triangular arrangements are antiferromagnetic in nature, this could lead to magnetic frustration in the system.

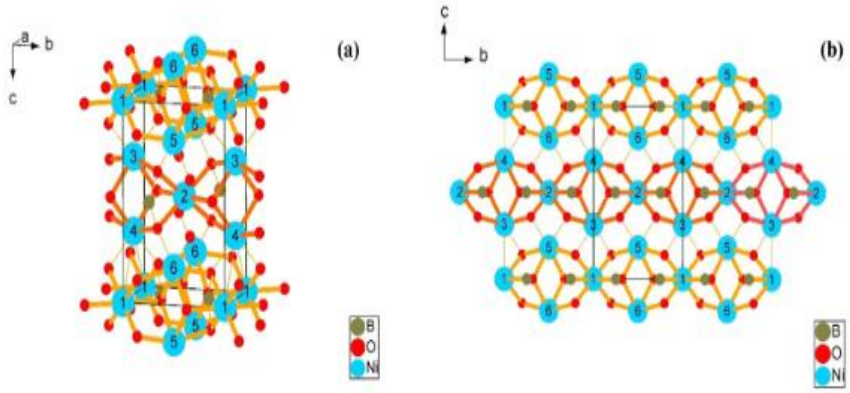

Figure 1.6 The unit cell of kotoite structure **(a)** perspective view **(b)** bc-plane view Bold lines show triangular groups in the bc plane. Ions 1,2 belong to crystallographic position 2a, ions 3-6 belong to position 4f.

Metal borate compounds hold significant industrial importance due to their magnetic properties, catalytic activities, and potential in optical applications. For instance, borates doped with various metals can emit UV, green, and red light, making them useful in medical lighting, fluorescent lamps, and plasma display technologies. Additionally, compounds such as β-BaB_2O_4 (BBO) and LiB_3O_5 (LBO) play an active role in laser systems.

Borates containing magnesium, cobalt, and nickel ($M_3(BO_3)_2$) typically crystallize in a mineral structure known as "kotoite." In this structure, metal ions are coordinated octahedrally with oxygen atoms, while boron atoms occupy trigonal planar positions. This hexagonally close-packed arrangement defines the characteristic properties of these compounds. The structure was first described by

researchers such as Götz, Pardo, and Effenberger. The figure shows the crystal structure of $M_3(BO_3)_2$ (M: Mg, Co, and Ni).

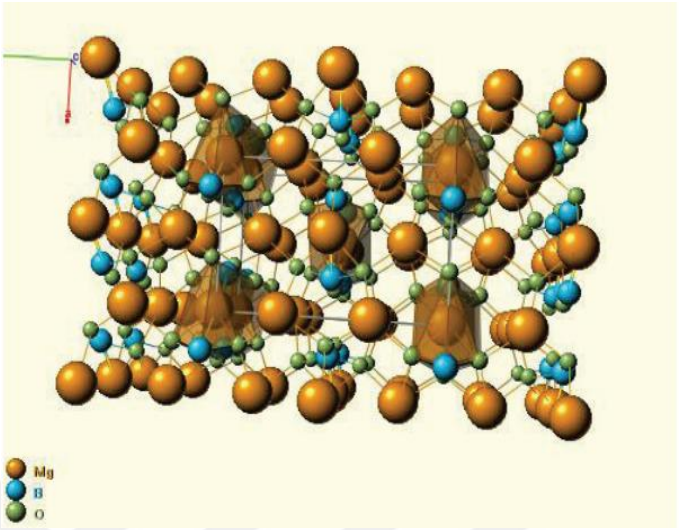

Figure 1.7 $M_3(BO_3)_2$ crystal structure

1.3 SYNTHESIS METHODS OF NICKEL BORATE

Nickel borate can be synthesized by several chemical and solid-state routes. Each method leads to different particle sizes, crystallinities, and morphologies. Below is a **highly detailed synthesis summary** extracted from a wide range of studies.

1. Solid-State Reaction Synthesis (Classic Ceramic Route)

Earliest known syntheses: 1960s–1970s (Pardo, 1974; Pertlik, 1975).

This remains one of the most reliable ways to obtain bulk crystalline $Ni_3(BO_3)_2$.

Typical Procedure

Precursors:

NiO (analytical grade) or $Ni(NO_3)_2 \cdot 6H_2O$ and H_3BO_3 (boric acid)

Stoichiometry:

$3\ NiO + 2\ H_3BO_3 \rightarrow Ni_3(BO_3)_2 + 3\ H_2O$

Conditions:

- Grinding/mixing: 1–3 h in agate mortar
- Calcination steps:

- **First calcination:** 500–600 °C for 4–6 h (to remove water)
- **Second calcination: 700–850 °C for 6–12 h** in air (to form $Ni_3(BO_3)_2$)

- **Final annealing:** Optional 900 °C for improved crystallinity (Pertlik, 1975)

Morphology:

- Dense crystalline powders, ~0.5–3 μm grain size.

Notes:

- Complete phase formation typically appears above **650 °C** (Ivanov et al., 2002).
- Above **950–1000 °C**, decomposition occurs and NiO reappears.

2. Hydrothermal Synthesis (Low-temperature Nanostructured Ni–B–O)

Hydrothermal synthesis yields **nanostructured** or **amorphous** nickel borate.

Example Hydrothermal Procedure (Chen et al., 2017)

Precursors:

$Ni(NO_3)_2 \cdot 6H_2O$, H_3BO_3 and Urea or NH_4OH (pH adjustment)

Conditions:

- pH adjusted to **7–9**
- Temperature: **160–200 °C**
- Autoclave duration: **12–24 h**
- Cooling naturally → washing and drying at 80 °C

Products: Amorphous Ni–B–O or nanocrystalline $Ni_3(BO_3)_2$ after calcination at **400–600 °C**

Example (Keles et al., 2014 — Surfactant Assisted)

- Surfactant: cetyltrimethylammonium bromide (CTAB)
- Ni precursor: $NiCl_2 \cdot 6H_2O$
- Borate source: $Na_2B_4O_7 \cdot 10H_2O$
- Hydrothermal treatment: **180 °C, 24 h**

Morphology:

- Nanorods (100–200 nm diameter)
- Hierarchical nanosheets/flower-like structures depending on surfactant ratio

3. Solvothermal Synthesis (Organic Solvents)

Solvents such as **ethylene glycol, glycerol, ethanolamine** can coordinate Ni^{2+} and control growth.

Typical Procedure

- Ni precursor: $Ni(CH_3COO)_2$ or $Ni(NO_3)_2$
- Borate precursor: trimethyl borate or boric acid
- Solvent: EG or DMF
- Temperature: **160–220 °C**
- Time: 6–18 h

This method produces **ultrafine amorphous films or nanoparticles** after low-temperature calcination.

4. Molten Salt Synthesis (Wang et al., 2015; Cao et al., 2014)

Used for **single-crystalline nanowhiskers**.

Procedure

Precursors:

- Ni plate substrate (acts as Ni source)
- Boric acid (H_3BO_3)
- Molten salt flux: NaCl–KCl eutectic (60/40 wt%)

Conditions:

- Mix boric acid + NaCl/KCl
- Place Ni substrate covered with mixture
- Heat at **850–950 °C** for **2–6 h**

Reaction:

Ni (from substrate) + BO_3^{3-} (from flux) → $Ni_3(BO_3)_2$ whiskers

Morphology:

- Nanowhiskers 150–300 nm diameter
- Length up to 20–50 μm
- At **>950 °C**, hollow microtubes may form due to vapor–solid growth (Cao et al., 2014)

5. Solution Combustion Method (Fast and Scalable)

Produces **nano-sized**, often porous Ni–B–O.

Example Procedure (Huang et al., 2018)

Precursors:

$Ni(NO_3)_2 \cdot 6H_2O$ (oxidizer) , H_3BO_3 (borate source) and Fuel: **glycine**, **citric acid**, or **urea**

Conditions:

- Precursor solution heated at ~80 °C → gel formation
- Sudden combustion at **250–350 °C**
- Final calcination at **500–700 °C** for crystallization

Fuel-to-oxidizer ratios strongly influence the particle size. Stoichiometric glycine–nitrate mixtures usually produce the highest-temperature combustion and the most porous final materials.

Example (Somanath et al., 2023)

- Temperature: combustion at 300 °C → annealing at **650 °C**
- Product: nanograins of $Ni_3(BO_3)_2$ (20–80 nm)

6. Co-precipitation + Calcination

Procedure

Precursors:

- $NiCl_2$ or $Ni(NO_3)_2$
- $Na_2B_4O_7$ or boric acid
- Base: NaOH or NH_4OH to pH ≈ 8–10

Steps:

1. Precipitation of $Ni(OH)_2$–$B(OH)_4^-$ gel
2. Drying at 100 °C
3. Calcination: **600–800 °C for 4–6 h**

Outcome:

- Good phase purity
- Sub-micrometer particles

7. Gelation / Sol-Gel Methods

Procedure

Precursors:

- $Ni(NO_3)_2$
- boric acid
- citric acid (chelating agent)

Conditions:

- pH: 3–7

- Gel formation at 80–100 °C
- Drying at 120 °C
- Calcination 500–700 °C → crystalline $Ni_3(BO_3)_2$

Morphology:

- Homogeneous nanoparticles ~20–50 nm

Characterization Techniques

A combination of structural, spectroscopic, microscopic, and electrochemical techniques is used to characterize nickel borates.

1. X-ray Diffraction (XRD)

XRD confirms the orthorhombic kotoite-type structure (space group: **Pnnm**).

Key reflections at ~2θ = 21–35° correspond to the (111), (112) and (121)planes (Pertlik, 1975; Cao et al., 2014; Wang et al., 2015).

Rietveld refinements (Knyazev et al., 2019) give typical lattice parameters:

- **a ≈ 5.39 Å**,
- **b ≈ 4.46 Å**,
- **c ≈ 8.29 Å**.

XRD also reveals crystallite size, phase purity, and decomposition signatures above 900 °C (Ivanov et al., 2002).

2. FTIR Spectroscopy

FTIR identifies internal vibrational modes of $[BO_3]^{3-}$:

- **ν_1 (symmetric stretching)** near ~930–970 cm^{-1}
- **ν_2 (bending)** around 700–760 cm^{-1}
- **ν_3, ν_4 (asymmetric)** near 1100–1350 cm^{-1}

Pisarev et al. (2015) observed phonon anomalies near the magnetic transition temperature, evidencing **strong spin–phonon coupling**.

3. UV–Vis Spectroscopy / Electronic Structure

Optical studies show that $Ni_3(BO_3)_2$ has a **band gap of ~4.8–5.3 eV**, larger than NiO due to the electron-deficient borate groups (Pisarev et al., 2015; Knyazev et al., 2019). Absorption spectra display characteristic **d–d transitions of Ni^{2+}** near 1.2 and 1.8 eV.

1.3.1 Solution Combustion Synthesis (SCS) Method

Solution-based methods are widely preferred due to their ability to produce high-purity products with small particle sizes. One such method, known as Solution Combustion Synthesis (SCS), was first introduced in 1967 through the work of Merzhano and colleagues. Over time, due to the large particle sizes and limited accessibility associated with the original method, it was combined with wet chemistry techniques and improved by Patil and coworkers, evolving into its current form.

SCS is based on an exothermic redox reaction, allowing for precise control over the composition and size of the resulting products. In this method, metal salts such as sulfates, nitrates, and carbonates are typically used as oxidizing agents, while organic compounds like urea, glycine, starch, or sucrose serve as reducing agents.

The synthesis process depends on several parameters, including the amount of water used in the starting solution, the type of fuel selected, the fuel-to-oxidizer ratio, the nature of the oxidizing agent, and the ignition temperature, which generally ranges between 300–500 °C. Among these, the amount of fuel plays a crucial role in determining the crystal structure and physical properties of the final product. An ideal fuel or oxidizer should have good solubility, be cost-effective, easily accessible, and possess a low decomposition temperature (Huang et al., 2018).

1.4 AIM AND SCOPE OF THE STUDY

The primary goal of this study is to successfully synthesize nickel orthoborate ($Ni_3B_2O_6$) using solution combustion synthesis (SCS), a cost-effective and relatively straightforward method. During the synthesis, reaction conditions will be optimized by employing various organic fuels, such as tartaric acid and

HMTA (hexamethylenetetramine). Additionally, the detailed effects of different post-synthesis heating temperatures on the crystal structure, crystallite sizes, and optical properties of the resulting nickel orthoborate will be investigated.

In the second phase of the study, the crystal structures of the synthesized orthoborates will be determined using X-ray diffraction (XRD) technique. Specifically, structural differences between the potential triclinic alpha and monoclinic beta forms of nickel orthoborate will be elucidated. Additionally, to predict whether the products exhibit nanosized particle structures, the crystallite sizes will be calculated using the Debye-Scherrer equation. These calculations will help us understand the influence of synthesis conditions on particle morphology.

Thirdly, the vibrational motions of the B-O bond within the triangular BO_3 groups in the nickel orthoborates will be assigned and analyzed using Fourier Transform Infrared (FTIR) spectroscopy. This will provide crucial insights into the compound's molecular structure.

2.MATERIALS AND METHODS

2.1 CHEMICALS

In this study, the chemicals used are listed below:

$Ni(NO_3)_2$, Nickel nitrate: Merck (pure 99.0%)

H_3BO_3, Boric acid: Merck, 99.00%

$C_4H_6O_6$, Tartaric acid : Merck, 99.00%

$C_6H_{12}N_4$, Hexamethylenetetramine (HMTA) : 99.90%

KBr, Potassium Bromide , for IR Spectroscopy : Merck, 99.90%

It was dried for 2 hours at 180^oC before using.

2.2 INSTRUMENTS

2.2.1 Furnace

The reactions during the preparation of metal borates and the annealing process were done by using Nuve MF 120 furnace in the range of 400-900oC.

Photo 2.1 The image of furnace

2.2.2 Fourier Transform Infrared Spectrophotometer

The infrared spectra and corresponding bond vibrations of the obtained products were analyzed using a PerkinElmer Fourier Transform Infrared (FT-IR) spectrophotometer, operating in the spectral range of 4000–400 cm^{-1}. For the measurements, the samples were prepared in pellet form by thoroughly mixing the product with potassium bromide (KBr) at a weight ratio of 0.1500:0.0010 (KBr: product, wt/wt), ensuring optimal transparency and uniform distribution for accurate spectral analysis.

Photo 2.2 Fourier Transform Infrared Spectrophotometer

2.2.3 X-Ray Powder Diffractometer

To examine the structural properties of the obtained compounds, the Rigaku miniflex and multiflex X-ray powder diffractometer illusrated in Photograph 3.4. with CuKα (30-40kV, 1020mA, λ=1,54056 Ǻ) radiation were used and the obtained data were compared with the ICDD data card.

Photo 2.3 The image of X-Ray Powder Diffractometer (XRD)

2.3 METHODS

The preparation of nickel orthoborates was successfully carried out using the SCS method. The starting materials were $Ni(NO_3)_2$ and H_3BO_3, with tartaric acid and HMTA serving as two different fuel types. $Ni(NO_3)_2$ and H_3BO_3 were used as the Ni and B sources, respectively.

2.3.1 Synthesis of Nickel Orthoborate

Nickel orthoborates were prepared using the solution combustion synthesis (SCS) method. Our starting materials, **$Ni(NO_3)_2$**, **H_3BO_3 (boric acid)**, and the fuels, **tartaric acid and HMTA**, were mixed in stoichiometric amounts and dissolved in a minimum amount of distilled water. The resulting mixture was continuously stirred on a magnetic stirrer at **370°C** until a gel-like consistency formed, allowing the water to evaporate.

The resulting gel-like structure was then held in a preheated furnace at **400°C for 5 minutes**. It was observed that the as-prepared product displayed different colors depending on the fuel types used. The annealing process was performed at two distinct temperatures: **400°C for 1 hour and 900°C for 1 hour**. Finally, the obtained products were characterized and compared.

Photo 2.4 The image of experimental procedure part of synthesis

Similar processes were carried out using **tartaric acid and HMTA** as fuels, and the expected reactions are presented below:

Tartaric Acid (TA)

$3Ni(NO_3)_2 + 2H_3BO_3 + 3C_4H_6O_6 \rightarrow Ni_3(BO_3)_2 + 12CO_2 + 3N_2 + 12H_2O$

HMTA

$18\ Ni(NO_3)_2 + 12H_3BO_3 + 5C_6H_{12}N_4 \rightarrow 6Ni_3(BO_3)_2 + 30CO_2 + 28N_2 + 48H_2O$

3. RESULTS AND DISCUSSION

3.1 The Solution Combustion Synthesis of Nickel Orthoborate ($Ni_3B_2O_6$)

In this study, the Solution Combustion Synthesis (SCS) technique was employed for the synthesis of nickel orthoborate compound. In the experimental studies, different organic fuels (hexamethylenetetramine and tartaric acid) were selected as one of the reaction parameters, and the process temperature was set within the range of 400-900°C. The reaction duration was determined to be one hour.

During the synthesis process, various physicochemical changes were observed in the system depending on the type of fuel used. Particularly notable were the observed gas emissions during combustion reactions and the resulting distinct differences in the color and morphological properties of the products. This demonstrates that the type of fuel used plays a determining role in the final product characteristics.

Tartaric Acid:

The homogeneous solution exhibited a turbid appearance and transformed into a green-colored gel at 370°C. A normal amount of gas was released during the process. After 5 minutes of preheating at 400°C, a rigid brown form was obtained.

a **b**

Photo 3.1 The images of $Ni_3B_2O_6$ samples prepared with tartaric acid fuel **a)** gel form **b)** synthesis

HMTA:

When the starting materials were dissolved in a small amount of distilled water, the resulting homogeneous solution was initially light green. However, as the temperature reached 370°C, a dark green, gel-like structure formed in the solution. The gas evolution observed during this process was at expected levels. Subsequently, after a 5-minute preheating stage at 400°C, the product turned a dark brownish-black color. Some difficulties were encountered when trying to remove this solidified product from the evaporating dish.

a **b**

Photo 3.2 The images of $Ni_3B_2O_6$ samples for HMTA fuel

a) gel form **b)** synthesis

3.1.1 Structural Characterization Studies of Nickel Orthoborate

The structural properties of nickel orthoborate were determined using products synthesized at 400°C for 10 minutes and subsequently heated at both 400°C and 900°C. Characterization was performed using X-Ray Diffraction (XRD) to examine the crystallite size and crystal structures, and FT-IR to identify the vibrational modes.

3.1.1.1. FT-IR Spectroscopy Studies

The FT-IR spectra of the synthesized by SCS technique, pure $Ni_3B_2O_6$ compound, as illustrated in Figures 3.1 to 3.6, reveal a series of distinct absorption bands corresponding to specific vibrational modes within the structure. These bands have been carefully analyzed and their assignments were made by comparing them with well-established vibrational data previously reported in the scientific literature [15], providing insights into the molecular structure and bonding environment of the borate compound.

The weak absorption bands assigned at 3431 cm^{-1} and 1635 cm^{-1} are most likely due to a small amount of physically adsorbed water on the surface of the sample, which is a common occurrence in metal borate materials exposed to ambient conditions.

A prominent and sharp band at 1303 cm^{-1} is attributed to the asymmetric stretching vibrations of the B(3)–O bonds, indicating the presence of BO_3 units in the crystal structure. Another strong absorption band appearing at 1186 cm^{-1} is tentatively assigned to the stretching vibrations of Ni–O bonds, suggesting strong metal–oxygen coordination within the lattice. Additionally, the absorption bands observed at 723 cm^{-1} and 633 cm^{-1} correspond to the out-of-plane bending modes of the B(3)–O groups, further confirming the exclusive presence of trigonal planar BO_3 units in the compound.

These vibrational band assignments are in excellent agreement with the expected structural features of nickel orthoborate, $Ni_3B_2O_6$, which is known to contain only BO_3 groups rather than tetrahedral BO_4 units, supporting the integrity and phase purity of the synthesized material.

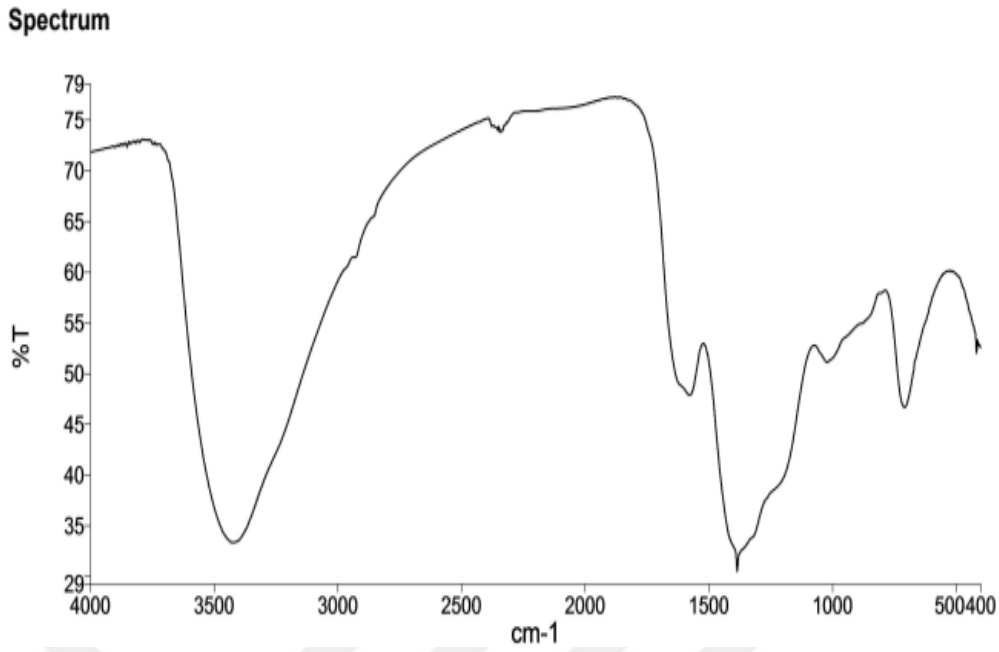

Figure 3.1 FT-IR Spectrum of as-prepared $Ni_3B_2O_6$, Using TA Fuel

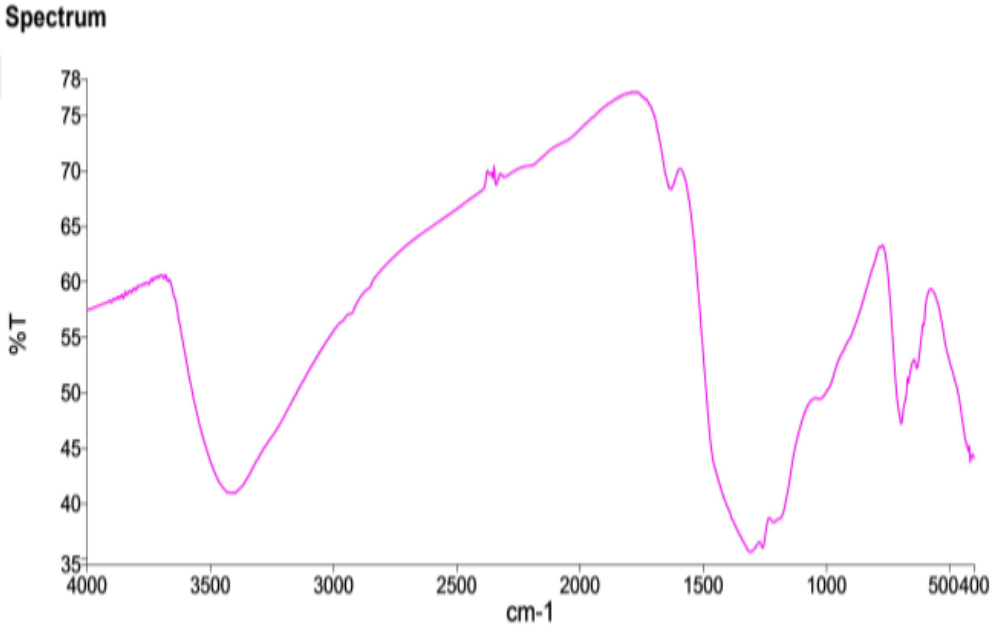

Figure 3.2 FT-IR Spectrum of as-prepared $Ni_3B_2O_6$, Using HMTA Fuel

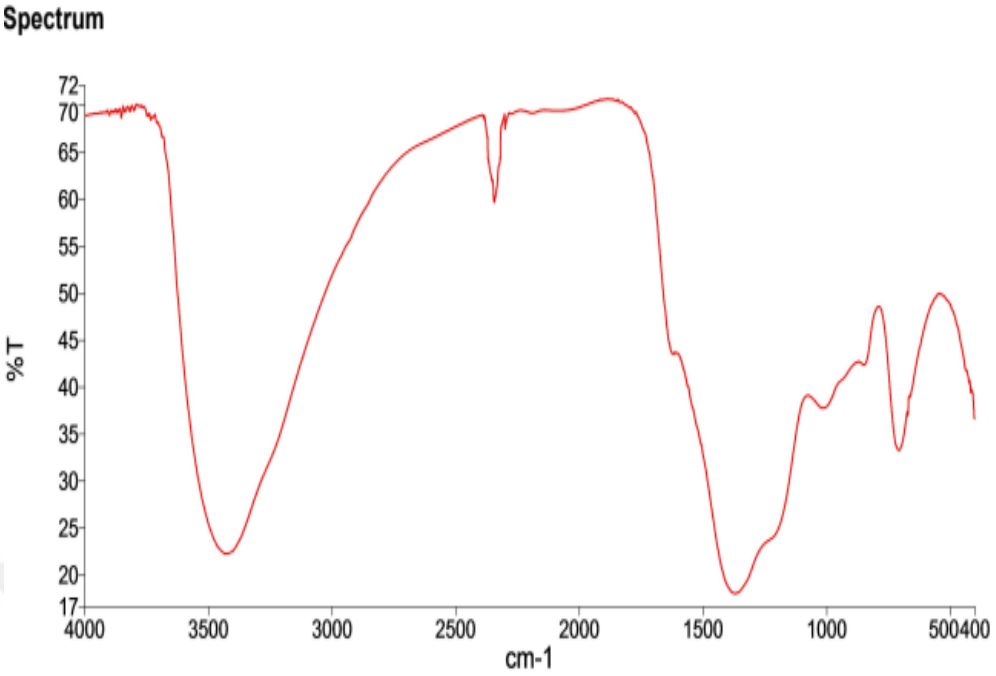

Figure 3.3 FT-IR Spectrum of $Ni_3B_2O_6$ heated at 400°C using TAFuel

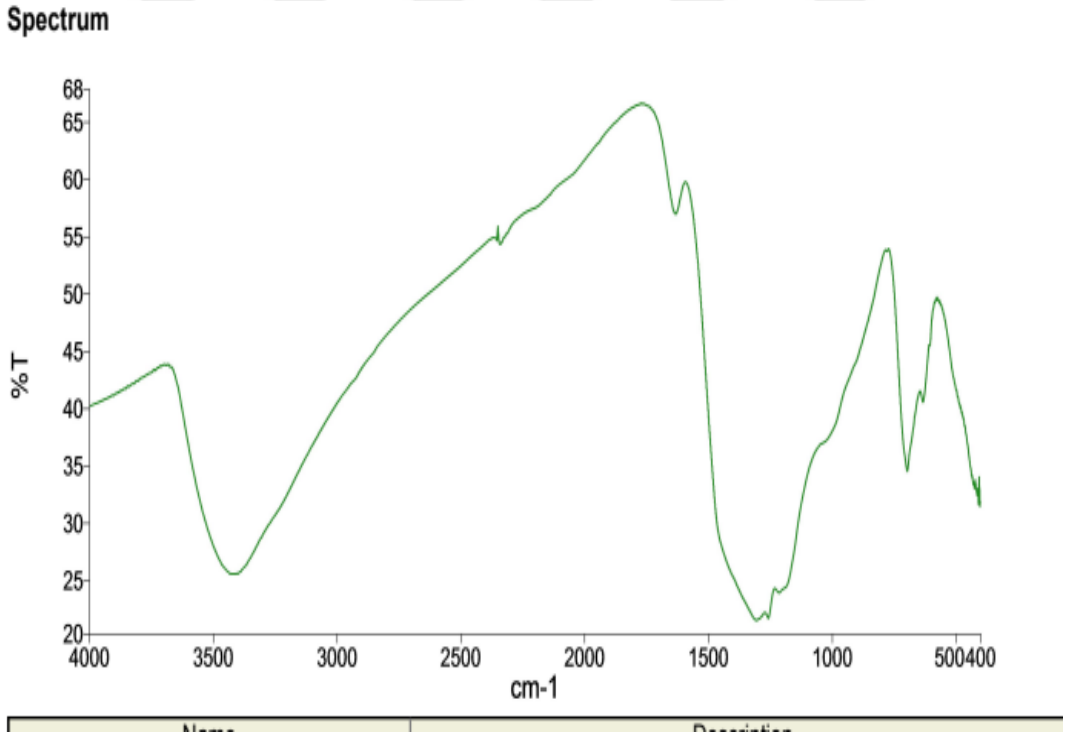

Figure 3.4 FT-IR Spectrum of $Ni_3B_2O_6$ heated at 400°C using HMTA Fuel

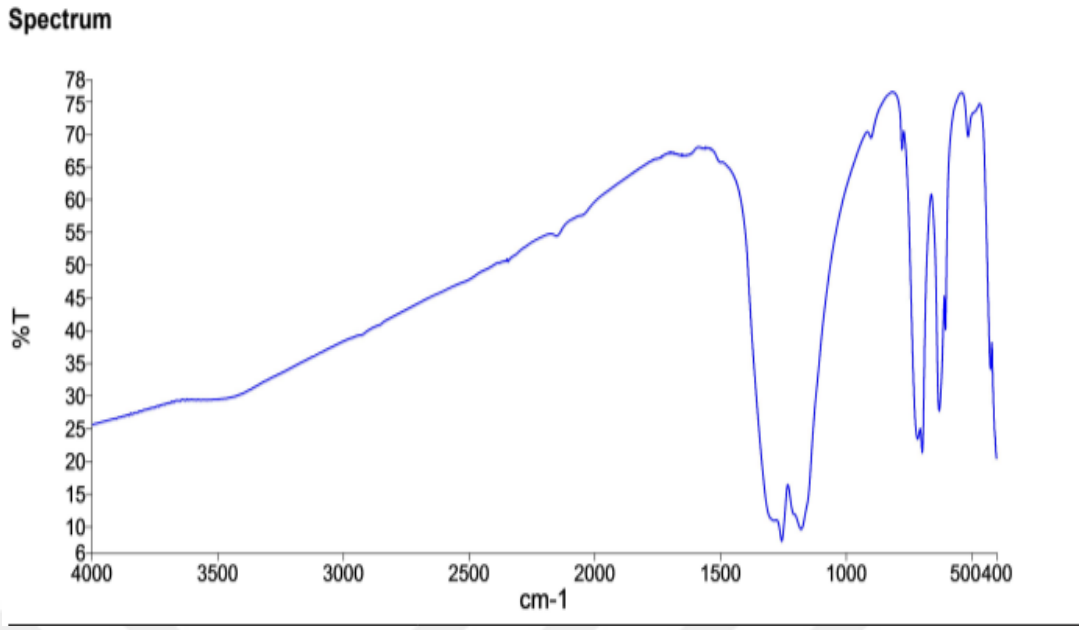

Figure 3.5 FT-IR Spectrum of $Ni_3B_2O_6$ heated at 900°C Using TA Fuel

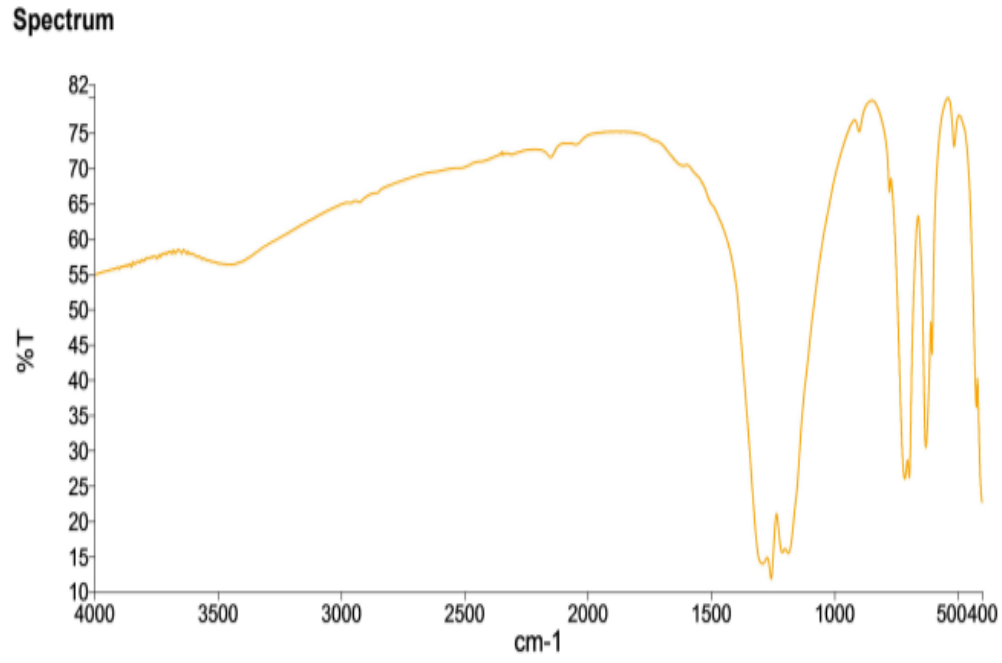

Figure 3.6 FT-IR Spectrum of $Ni_3B_2O_6$ heated at 900°C Using HMTA Fuel

3.1.1.2 X-Ray Diffraction (XRD) Studies

The crystallinity and phase composition of the synthesized $Ni_3B_2O_6$ material were thoroughly investigated using powder X-ray diffraction (XRD) analysis. This technique was employed to examine the structural evolution of the as-prepared nickel orthoborate samples subjected to calcination at different temperatures.

The XRD patterns corresponding to the samples sintered at 400 °C and 900 °C, utilizing TA and HMTA as fuels, are presented in Figures 3.7 and 3.8, respectively. At the relatively low calcination temperature of 400 °C, the recorded diffraction pattern revealed a broad and diffuse background without any distinct peaks, indicating the presence of an amorphous phase and suggesting that the crystallization process had not yet commenced at this stage. However, upon increasing the calcination temperature to 900 °C, a significant transformation in the phase structure was observed. Well-defined and sharp diffraction peaks emerged, signifying the formation of a highly crystalline material.

The peak positions and intensities clearly indicated the successful synthesis of phase-pure $Ni_3B_2O_6$ with no detectable secondary phases. This observation confirms that 900 °C is a sufficient temperature for complete crystallization and phase stabilization of $Ni_3B_2O_6$.

The XRD powder diffraction patterns obtained at 900 °C exhibited characteristic reflections at 2θ values of 22.6°, 25.8°, 33.8°, 36.7°, 40.5°, 43.3°, 53.2°, 55.5°, 59.5°, 62.2°, and 69.5°, which correspond to the (011), (101), (121), (211), (131), (040), (202), (132), (321), (330), and (251) crystallographic planes, respectively. These diffraction peaks are in excellent agreement with those of orthorhombic $Ni_3B_2O_6$, and all observed reflections can be successfully indexed to this structure based on the Joint Committee on Powder Diffraction Standards (JCPDS) card No. 22-0745. The data conclusively confirm that the product obtained at 900 °C exhibits a single-phase orthorhombic crystal structure with high crystallinity, demonstrating the efficiency of the calcination process in promoting phase formation and structural ordering.

In addition to confirming the formation of orthorhombic $Ni_3B_2O_6$ at elevated temperatures, further analysis of the XRD data provides valuable insight

into the material's structural characteristics. The sharpness and intensity of the diffraction peaks obtained at 900 °C indicate a high degree of crystallinity, which reflects the enhanced atomic ordering within the lattice as a result of sufficient thermal energy during the calcination process. The absence of any secondary phases or impurity peaks across the entire diffraction pattern further confirms the high phase purity of the synthesized product.

To estimate the average crystallite size of the $Ni_3B_2O_6$ particles, the Scherrer equation was applied to the most intense diffraction peak, typically located around $2\theta \approx 33.8°$, corresponding to the (121) plane. The calculated crystallite size was found to be in the nanometer range, suggesting that while the material exhibits high crystallinity, it still retains a fine microstructure, which may be advantageous for various applications, such as catalysis or electrochemical energy storage, due to the increased surface area.

Moreover, a comparative assessment of the XRD patterns obtained using different fuels—Tartaric Acid (TA) and Hexamethylenetetramine (HMTA)—reveals subtle differences in peak broadening and relative intensities. Samples synthesized using HMTA as fuel tend to exhibit slightly narrower and more intense peaks compared to those prepared with TA, implying a marginally higher crystallinity and possibly larger crystallite domains. This observation can be attributed to differences in combustion behavior: HMTA, being a nitrogen-rich compound, generally promotes a more uniform and energetic combustion process, thereby enhancing thermal decomposition and crystal growth during synthesis.

Additionally, the unit cell parameters of orthorhombic $Ni_3B_2O_6$ allow a more quantitative assessment of the lattice distortions and potential substitutional defects, if present. Such structural details are critical for understanding the influence of synthesis conditions on the final properties of the borate material.

In summary, XRD analysis confirms that calcination at 900 °C results in the successful formation of phase-pure, orthorhombic $Ni_3B_2O_6$ with well-developed crystallinity. The choice of fuel plays a secondary but noticeable role in crystallite growth and structural uniformity. These findings highlight the importance of thermal treatment parameters and fuel chemistry in directing the structural evolution and phase purity of metal borate materials.

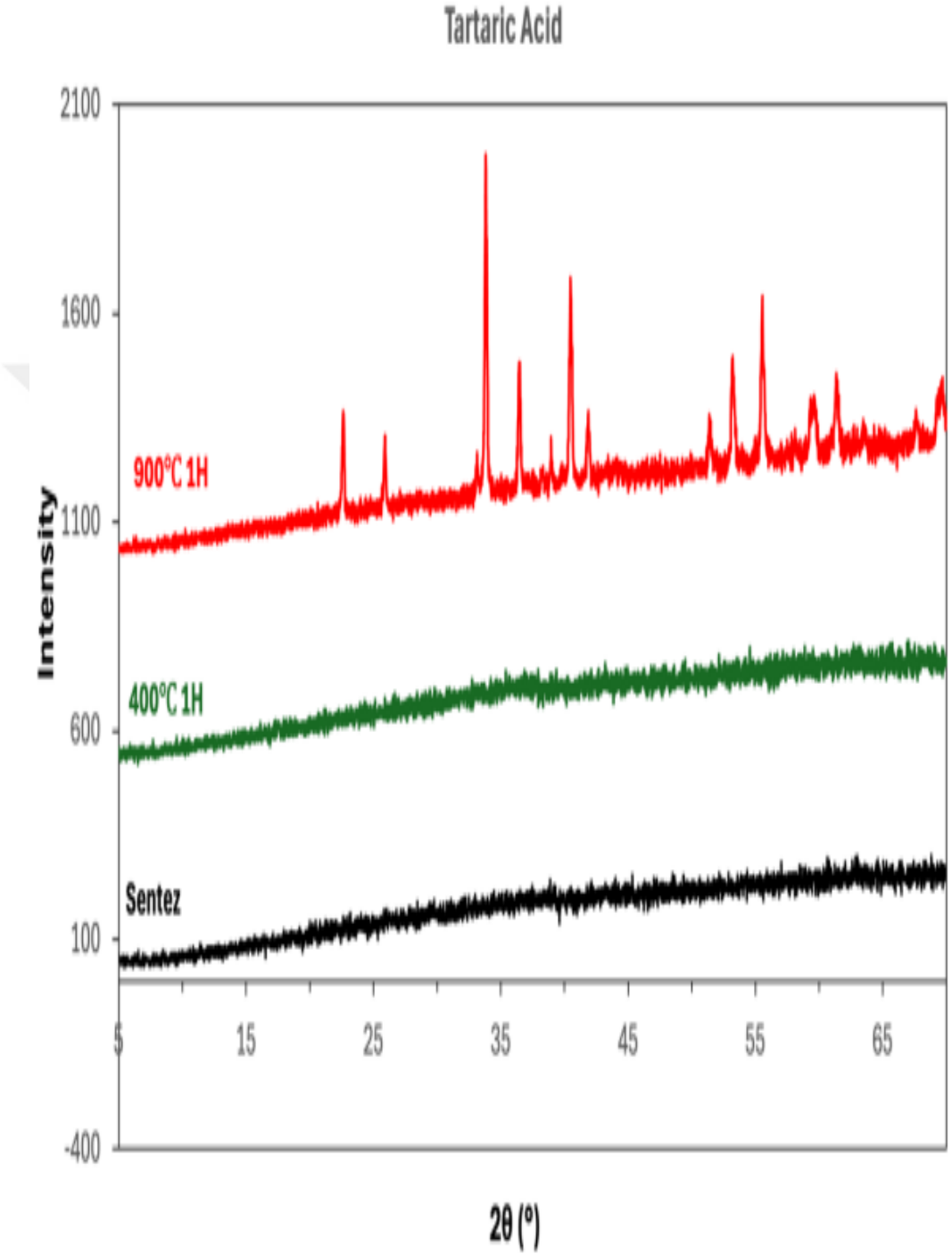

Figure 3.7 XRD Patterns of $Ni_3B_2O_6$ produced by SCS method Using TA Fuel

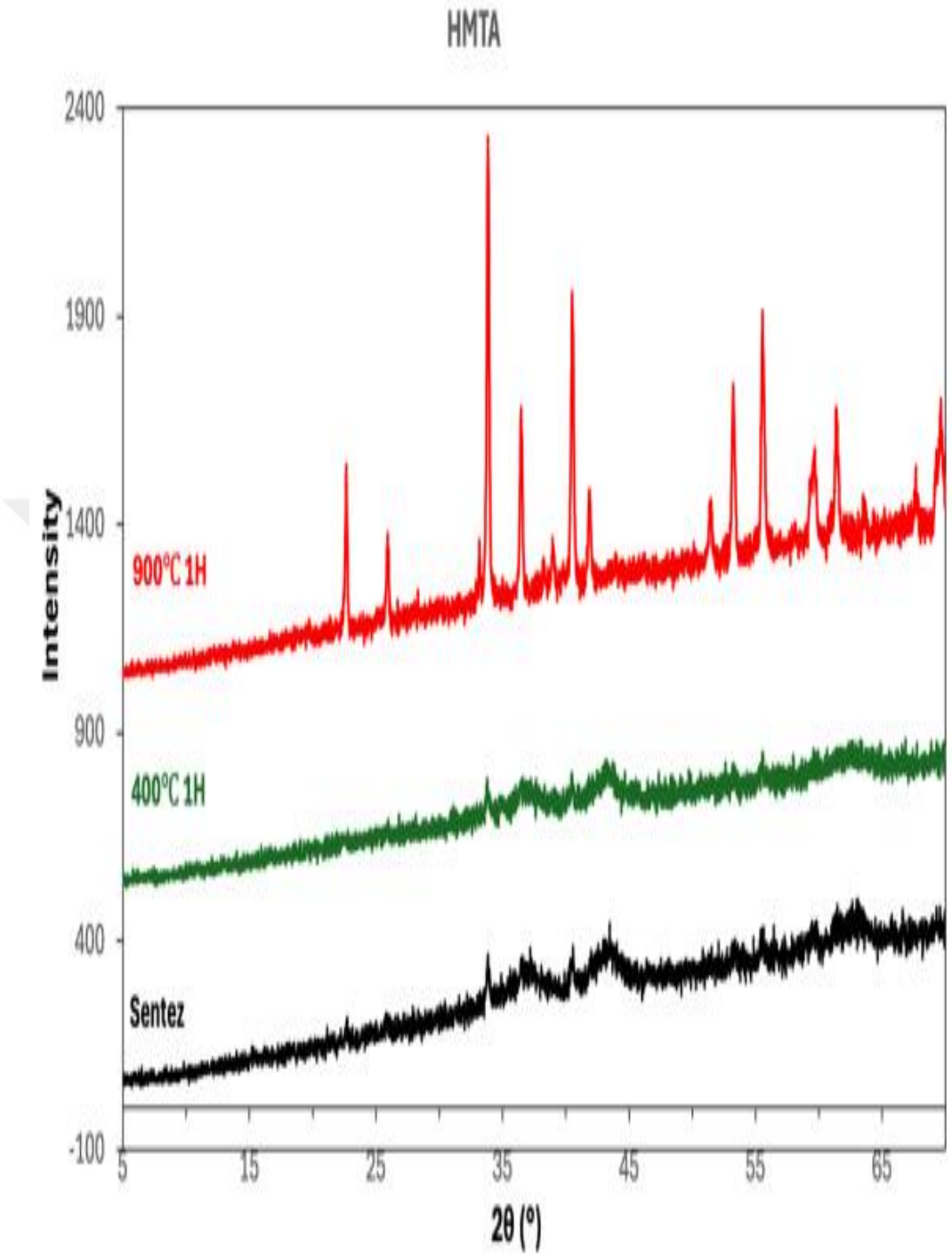

Figure 3.8 XRD Patterns of $Ni_3B_2O_6$ produced by SCS method Using HMTA Fuel

4. CONCLUSION

Nickel orthoborate ($Ni_3(BO_3)_2$) was successfully synthesized using both tartaric acid (TA) and hexamethylenetetramine (HMTA) as fuels via the solution combustion synthesis (SCS) method. The reactions were efficiently carried out with short processing times and at moderate temperature ranges (400-900°C). Stoichiometric calculations and experimental masses (0.9631 g for TA and 0.7988 g for HMTA) confirmed the expected yields, with a 4% excess of H_3BO_3 ensuring complete reaction.

XRD analyses revealed distinct phase formations at different temperatures. At 400°C, amorphous or low-crystallinity phases were dominant, while at 900°C, well-crystallized ($Ni_3(BO_3)_2$) phases characterized by sharp diffraction peaks were observed. The enhancement of phase purity through thermal treatment was supported by TGA data showing weight losses of 0.0228 g for TA and 0.0072 g for HMTA after 1-hour heating.

FT-IR spectra confirmed the presence of BO_3 groups through bands at 695-720 cm^{-1} (bending), 1010-1065 cm^{-1} (symmetric stretching), and 1220-1245 cm^{-1} (asymmetric stretching). HMTA-derived samples exhibited sharper peaks at 900°C, indicating better structural ordering compared to TA.

This study demonstrates that HMTA is more suitable for producing high-crystallinity products, highlighting the versatility of the SCS method for ($Ni_3(BO_3)_2$) synthesis. Future studies should focus on improving properties for functional applications and optimizing environmentally friendly synthesis protocols.

REFERENCES

Anadolu Agency. (2025, January 15). *Turkey projects to generate $1 billion in boron exports in the next 10 years*. https://www.aa.com.tr/en/energy/finance/turkey-projects-1-bln-exports-with-boron-in-10-years/8625

Bediako, D. K., et al. (2012). Structure–activity relationships in nickel–borate oxygen evolution catalysts. *Journal of the American Chemical Society, 134*(15), 6801–6809.

Bengisu, M. (2016). Borate glasses for scientific and industrial applications: A review. *Journal of Materials Science, 51*, 2199–2242. https://doi.org/10.1007/s10853-015-9537-4

Britannica. (2025). *Boron | Properties, uses, & facts*. Encyclopædia Britannica. https://www.britannica.com/science/boron-chemical-element

Cao, J., Wang, Y., Song, X., & Feng, J. (2014). One-dimensional nickel borate whiskers. *RSC Advances, 4*, 19295–19301.

Chen, L., et al. (2017). Hydrothermal synthesis of nickel borate nanostructures. *Materials Chemistry and Physics, 192*, 59–67.

Christ, C. L., & Clark, J. R. (1977). Crystallography of borates. *American Mineralogist, 62*, 398–413.

Demiral Kurtuluş, F., & Güler, H. (2003). Synthesis of some metal containing borate and boron phosphate compounds by solid-state methods. *Journal of Balikesir University Institute of Natural and Applied Sciences, 5*(1), 141–152.

Ede, S. R., et al. (2018). Microwave-assisted synthesis of $Ni_3(BO_3)_2$ nanostructures. *Energy & Fuels, 32*, 8800–8807.

Effenberger, H. (1971). Orthoborates of transition metals. *Acta Crystallographica B, 27*, 785–792.

Effenberger, H., & Pertlik, F. (1984). Verfeinerung der Kristallstrukturen der isotypen Verbindungen $M_3(BO_3)_2$ (M = Mg, Co, Ni). *Zeitschrift für Kristallographie, 166*, 129–136.

Enez, S., et al. (2023). Co-doped nickel borate for OER. *ChemistrySelect, 8*, e202203561.

European Borates Association (EBA). (2011). *Borates*. IMA-Europe. http://www.ima-europe.eu

Eti Maden. (n.d.-a). *Boron in the world*. https://www.etimaden.gov.tr/en/boron-in-the-world

Eti Maden. (n.d.-b). *Boron in Turkey*. https://www.etimaden.gov.tr/en/boron-in-turkey

Ganguly, A. K., Sharma, S., Menaka, Ramanujachary, K. V., & Lofland, S. E. (2011). Controlling the size and morphology of anisotropic nanostructures of nickel borate using microemulsions. *Journal of Colloid and Interface Science, 360*(2), 393–397.

Gül, E. (2013). *Synthesis and characterization of novel mixed-metal orthoborates* (Master's thesis). Abant İzzet Baysal University.

Guo, R., et al. (2021). Z-scheme g-C_3N_4/NiO/$Ni_3(BO_3)_2$ photocatalyst. *Journal of Photochemistry and Photobiology A, 407*, 113080.

Heller, G., & Dunham, D. (1984). Borate structural chemistry. *Journal of Solid State Chemistry, 51*, 112–125.

Helvacı, C. (2019). Turkish borate deposits: Geological setting, genesis and overview of the deposits. In *Mineral resources of Turkey*. Springer.

Huang, Q., et al. (2018). Combustion-derived Ni–B–O catalysts. *Ceramics International, 44*, 20241–20249.

Huang, Z., Wang, S., Dewhurst, R. D., Ignat'ev, N. V., Finze, M., & Braunschweig, H. (2020). Boron: Its role in energy-related processes and applications. *Angewandte Chemie International Edition, 59*(23), 8800–8816.

Ivanov, V., et al. (2002). Thermal stability of nickel borates. *Thermochimica Acta, 394*, 71–78.

Kar, Y., Sen, N., & Demirbaş, A. (2006). Boron minerals in Turkey, their application areas and importance for the country's economy. *Minerals and Energy, 20*, 2–10.

Keles, E., et al. (2014). Hydrothermal synthesis of nickel borate. *Journal of Nanoscience and Nanotechnology, 14*, 1234–1240.

KimyaKongreleri.org. (2011). *Magnezyum nikel ortoborat bileşiğinin sentezi ve karakterizasyonu*. http://kimyakongreleri.org/2011/2011-224.pdf

Knyazev, A. V., et al. (2019). Optical constants and electronic properties of $Ni_3(BO_3)_2$. *Optical Materials, 93*, 44–51.

Liang, P., Du, L., Wang, X., & Liu, Z.-H. (2014). $Ni_3B_2O_6$ nanosheet-based architecture via precursor method. *Solid State Sciences, 37*, 131–135.

Mariselvam, K., & Arun Kumar, R. (2016). Borate glasses for luminescence applications. *Universal Journal of Chemistry, 4*(2), 55–64.

Molchanova, A. D. (2018). Absorption spectra of Ni^{2+} ions in $Ni_3(BO_3)_2$. *Physics of the Solid State, 60*(10), 1957–1965.

Öztürk, M. (2023). *The influence of synthesis conditions on nanosized zinc orthoborates* (Master's thesis). Abant İzzet Baysal University.

Pang, H., Lu, Q., Chen, C., Liu, X., & Gao, F. (2011). $Ni_3(BO_3)_2$ nanoribbons: Properties and synthesis. *Journal of Materials Chemistry, 21*, 13889–13894.

Pardo, J. (1974). The crystal structure of nickel orthoborate. *Acta Crystallographica B, 30*, 29–31.

Pertlik, F. (1975). Orthoborates of Mg, Co, Ni. *Monatshefte für Chemie, 106*, 509–518.

Pisarev, R. V., Prosnikov, M. A., Davydov, V. Yu., Smirnov, A. N., Roginskii, E. M., Boldyrev, K. N., … Kazimirov, V. Yu. (2015). Lattice dynamics of $Ni_3(BO_3)_2$. *Physical Review B, 92*, 134306.

Pisarev, R. V., et al. (2015). Lattice dynamics and a magnetic-structural phase transition in $Ni_3(BO_3)_2$. *arXiv*. https://doi.org/10.48550/arXiv.1509.00344

Priyam Study Centre. (2020, November). *Boron*. https://www.priyamstudycentre.com/2020/11/boron.html

Republic of Türkiye Ministry of Energy and Natural Resources. (2024). *Boron*. https://www.enerji.gov.tr/infobank-naturalresources-boron

Rodriguez-Hernandez, P., et al. (2018). Raman modes of orthoborates. *Journal of Raman Spectroscopy, 49*, 1120–1129.

Sanglay, G. D. D., Garcia, J. S., Palaganas, M. S., Sorolla, M. II, See, S., Limjuco, L. A., & Ocon, J. D. (2022). Borate-based compounds for advanced batteries. *Molecules, 27*(22), 8047.

Singh, S., Srinivas, B., & Ram, S. (2008). Nickel borate: Synthesis and properties. *Journal of Solid State Chemistry, 181*(12), 3368–3373.

Sofronova, S. N., & Nazarenko, I. I. (2019). Super-superexchange in $Ni_3B_2O_6$ Kotoite. *Physica Status Solidi B, 256*(10), 1900060.

Sokmen, N., & Büyükakinci, B. Y. (2018, March 21–23). *The use of boron/boron compounds in the textile industry and their use in Turkey*. CBU International Innovation Conference, Prague.

Somanath, B., et al. (2023). Combustion synthesis of $Ni_3(BO_3)_2$. *ACS Applied Energy Materials, 6*, 4211–4220.

Sun, X., et al. (2022). Electrodeposition of $Ni_3(BO_3)_2$ nanospheres. *Journal of Energy Storage*. https://doi.org/10.1016/j.est.2022.105445

Universalium. (2025). *Some properties of the boron group elements*. https://universalium.enacademic.com/295125

Wang, Y., Feng, J., Feng, B., Song, X., & Cao, J. (2015). Molten-salt growth of nickel borate nanowhiskers. *RSC Advances, 5*, 28950–28957.

Yamamoto, H., Miyata, A., & Koyama, K. (2006). Gibbs energy of $Ni_3B_2O_6$ formation. *Journal of the Japan Institute of Metals and Materials, 70*(3), 233–237.